RSC Advances

PAPER

View Article Online
View Journal | View Issue

Cite this: *RSC Adv.*, 2019, **9**, 3693

Green and facile production of high-quality graphene from graphite by the combination of hydroxyl radicals and electrical exfoliation in different electrolyte systems

Xin Wang [ab] and Long Zhang *[a]

A novel, simple and efficient method by the combination of hydroxyl radicals and electrical exfoliation of graphite for the green production of high-quality graphene from graphite was first developed in our self-manufactured exfoliation apparatus. In this work, we focused on the investigation of the roles of various electrolyte systems for the exfoliation of graphite. Sodium chloride, sodium hydroxide, poly vinyl pyrrolidone (PVP), dodecyl trimethyl ammonium bromide (DTAB) and sodium dodecyl benzene sulfonate (SDBS) were tested as the electrolyte. The yields of the graphene product in sodium hydroxide, PVP, DTAB, sodium chloride and SDBS electrolyte system were 32.9%, 34.0%, 45.2%, 77.5% and 83.5%, respectively. The experimental result demonstrated that graphite can be successfully exfoliated to graphene in these electrolytes, with SDBS showing the best exfoliation effect. We further investigated the effects of process parameters on the graphite exfoliation in the SDBS system by single factor experiments. The obtained optimal process parameters were as follows: graphite dosage, 5.0 g; SDBS solution concentration, 10.0% (w/v); applied current strength, 10 mA; air flow, 1.0 L h^{-1}; and exfoliation time, 3 h. At these conditions, the yield of the graphene product was 89.7%. TEM results revealed that the graphene product possessed the characteristic features of a thin-layer graphene sheet. XRD results showed that the graphene products still maintained the structures of carbon atoms or molecules. FT-IR and Raman results indicated that the products exhibited the characteristic peaks and the absorption peaks of graphene. AFM test results revealed that the layer number of graphene product obtained was about 2, while the layer numbers of the graphene products obtained from sodium hydroxide, PVP, DTAB and sodium chloride systems were 30, 20, 4 and 3, respectively, at the same experimental conditions. The observed exfoliation effect in the SDBS system was due to its good electrical conductivity, which was favorable for the formation of hydroxyl radicals in exfoliation. Furthermore, SDBS has good hydrophilic properties and can enable even dispersion of graphite in the system. These two effects facilitated the exfoliation of graphite to form good-quality graphene. SDBS as the electrolyte did not corrode the electrode, and it could be recycled; also, it does not pollute the environment and reduces the production cost, which is favorable for mass production.

Received 27th November 2018
Accepted 10th January 2019

DOI: 10.1039/c8ra09752f

rsc.li/rsc-advances

1. Introduction

Graphene is the latest member of the nano-carbon family with a two-dimensional honeycomb lattice structure of closely stacked carbon atoms in a single layer.[1] It exhibits many special physicochemical properties such as strong mechanical properties,[2] high electrical conductivity,[3] high barrier properties[4] and good catalytic properties.[5] Due to these properties, graphene shows numerous application potentials in many fields. Since Geim *et al.*[6] obtained a single layer of graphene by mechanical stripping in 2004, many other methods for preparing graphene have also been developed. At present, the most popular methods for the preparation of graphene include micro-mechanical stripping,[7–11] ball milling,[12–14] chemical vapor deposition,[15–18] solvothermal method,[19–21] liquid phase exfoliation[22,23] and oxidation–dispersion.[24–29] The above preparation methods often employ aggressive reagents and are restricted by the relatively high energy consumption, complex operation, environmental pollution, occasional low yields and poor product quality. Electrochemical exfoliation has been widely studied since it can be easily operated and can be employed to obtain a graphene product from graphite.[30–32] Sahoo *et al.*[30]

[a]*Jilin Provincial Engineering Laboratory for the Complex Utilization of Petro-resources and Biomass, School of Chemical Engineering, Changchun University of Technology, Changchun, Jilin, 130012, P. R. China. E-mail: zhanglongzhl@163.com; Tel: +86 18686672766*

[b]*School of Petrochemical Technology, Jilin Institute of Chemical Technology, Jilin, 132022, P. R. China*

reported graphene preparation with concentrated sulfuric acid solution as the electrochemical exfoliation electrolyte to produce 4–6 layered graphene sheets. Chakrabarti *et al.*[32] conducted a similar research with an ionic liquid, eutectic solvent and acetonitrile electrolyte to obtain a graphene sheet of 4–5 layers. However, the use of organic solvents and inorganic strong acids often leads to environmental problems and increases the production expense; also, the product quality is not satisfactory. Therefore, it is necessary to develop a novel greener production method to resolve the problems mentioned above.

Hydroxyl radicals have a standard oxidation–reduction potential of 2.8 V, which is only lower than that of F.[33] They can react with many organic molecules due to their strong oxidation capacity. Moreover, hydroxyl radicals can initiate and transfer the chain reaction as well as oxidize and decompose organic substances into less toxic or non-toxic small molecules. The most commonly used methods to generate hydroxyl radicals include Fenton reaction,[33] Haber–Weiss reaction[34] and electrochemical methods.[35,36] These hydroxyl radical generation methods have the disadvantages of higher energy consumption and complex production procedures; also, they are not suitable for mass applications. The hydroxyl radicals are mainly used in the fields of sewage treatment, sterilization, food and vegetable preservation and carbon nanotube modification.[34–36] G. Feng *et al.*[37] introduced ·OH (produced by UV light irradiation) into the synthetic process of zeolite for the first time, and the experimental results showed that ·OH could significantly accelerate the nucleation of zeolite, thereby accelerating its crystallization process. However, there is no report on the application of hydroxyl radicals used for graphite exfoliation to prepare graphene.

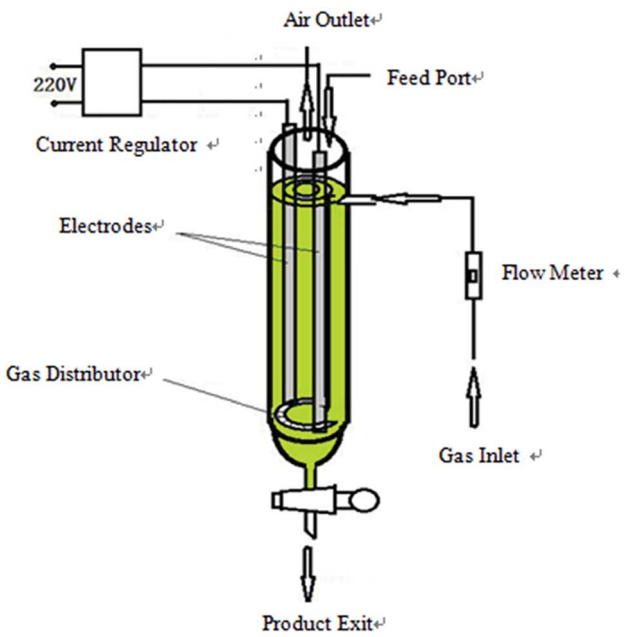

Fig. 1 The diagram of hydroxyl radical generation and graphite exfoliation apparatus.

In our previous research,[38] for the first time, we successfully used hydroxyl radical exfoliation for the facile and green production of high-quality graphene from graphite with sodium chloride as the electrolyte in our self-manufactured device; also, the graphite was successfully exfoliated to graphene sheets. Considering the key roles of the electrolyte in the exfoliation process, PVP, SDBS, DTAB, *etc.* were widely[39–43] tested, and they exhibited better dispersion and stabilization functions. In this work, we compared the effects of different electrolyte systems on the exfoliation of graphite to find a suitable electrolyte. To achieve this goal, experiments with sodium chloride, sodium hydroxide, PVP, DTAB and SDBS as the electrolytes were carried out. The effects of process parameters (such as exfoliation time, electrolyte concentration, graphite dosage, applied current strength and air flow) on the production of graphene were investigated using SDBS as the suitable electrolyte. The experimental results proved that graphite was successfully exfoliated into the graphene product. The layer number of graphene obtained in the SDBS electrolyte system was about 2, while the layer numbers of graphene products in sodium hydroxide, PVP, DTAB and sodium chloride electrolytes were 30, 20, 4 and 3, respectively, at the same experimental conditions.

2. Experimental

2.1 Materials and instruments

Flake graphite (carbon content of 97%, moisture content of less than 0.5%, density of 1.6 g cm^{-3}, flake size of 0.5 mm) was purchased from Sinopharm Chemical Reagent Co., Ltd. (Shanghai, China). Sodium chloride (AR), sodium hydroxide (AR), poly vinyl pyrrolidone (PVP) (AR), dodecyl trimethyl ammonium bromide (DTAB) (AR), sodium dodecyl benzene sulfonate (SDBS) (AR) and ethanol (AR) were all purchased from Sinopharm Chemical Reagent Co., Ltd. (Shanghai, China).

The hydroxyl radical production and graphite exfoliation apparatus was designed and manufactured by our laboratory, and the detailed device diagram is shown in Fig. 1. An analytical balance (TG328A) was purchased from Balance Instrument Factory (Shanghai, China). The pumping equipment was purchased from Guohua Electric Co. (Shanghai, China). The vacuum drying oven was purchased from Anteing Electronic Instrument Factory (Shanghai, China).

2.2 Experimental devices

This device is a high efficiency hydroxyl radical generation apparatus. The apparatus consists of a current regulator, an electrode system, a gas inlet and a distributor, a flow meter, a feed port, an air outlet and a product exit. The reaction liquid (water and electrolyte) and graphite were added from the feed port. The air flow rate was adjusted by a flow meter. The air and graphite were evenly distributed in the reaction medium under the action of the air distributor, and the intensity of the applied current was adjusted by the current regulator. When an electric current was applied, water was decomposed and oxidized to produce ·OH in the reactor with graphite as the catalyst, and the

formed ·OH subsequently reacted with graphite to produce graphene.

After the completion of exfoliation, graphene was removed from the product exit, filtered, and washed with distilled water and dried (60 °C for 18 hours) to get the product. The diagram of the apparatus is shown in Fig. 1.

2.3 Preparation procedures

Graphite powders were loaded into the hydroxyl radical apparatus containing a volume of SDBS solution according to the experimental design. The applied current strength in the process was adjusted by a variable resistor having 50–500 Ω. The exfoliation experiments were started when the electric current was applied; the electrode oxidatively decomposed the water to produce ·OH in the reactor with graphite as the catalyst, which subsequently reacted with graphite to produce graphene. The graphite added to the reaction liquid also served as a catalyst, due to which the generation of hydroxyl radicals and the reaction between the hydroxyl radicals and the graphite in the solution occurred simultaneously. After the designed exfoliation time, the solution was filtered and washed and the solid was dried (60 °C for 18 hours) and ground to powder for characterization; the filtrate was reused for the next experiment.

To compare the effects of different electrolyte systems on exfoliation, experiments with sodium chloride, sodium hydroxide, PVP, SDBS and DTAB as the electrolytes were carried out. Then, we chose the suitable electrolyte system for further process optimization. Five process factors (exfoliation time, electrolyte concentration, graphite dosage, applied current strength and air flow) were designed and tuned in the exfoliation.

2.4 Characterization

2.4.1 Morphological elucidation. Morphological information of the samples was obtained by a H800 transmission electron microscope (Tokyo, Japan). Further morphological information was obtained by an atomic force microscope.

2.4.2 Structural investigation. The molecular structure of the graphene product obtained was identified by X-ray diffraction. After vacuum drying and grinding to powders, samples were scanned and recorded using an X-ray diffractometer (Rigaku, Japan) with an X-ray generator from 15 to 60 of 2θ (diffraction angle) using Cu/Kα irradiation at 55 mA and 60 kV. The structural information of the product was obtained by Raman (Horiba JY) and FT-IR spectroscopy. Fourier transform infrared (FT-IR) spectra were obtained with an IS50 FT-IR system spectrometer (Horiba JY). The scanned wave number range was 4000–400 cm^{-1}. After vacuum drying and grinding to powders, the powders and KBr were compacted into disks and analyzed.

2.4.3 Product yield determination. The graphene dispersion has a good Lambert–Beer behavior, and the concentration of the graphene dispersion has a good linear relationship with the ultraviolet absorbance. $A/I = \alpha C$, where A/I is the absorbance value of the unit cuvette length, C is the concentration of the graphene dispersion, and α is the extinction coefficient of the graphene dispersion. A large number of studies have reported that the ultraviolet characteristic detection wavelength of graphene is 660 nm, and graphite has no absorption peak here. It is reported[44] that the extinction coefficient $(\alpha) = 3620\ L^{-1}\ g^{-1}\ m^{-1}$ for the graphene dispersion at $\lambda = 660$ nm. The dosage of graphite was 4.0 g, and the reaction liquid was 1.0 L in the above experiments. The reaction solution after exfoliation (quiescent for 2 hours) was diluted and then subjected to ultraviolet detection at 660 nm. The yields of the product were calculated by the following eqn (1). Under optimal conditions, the dosage of graphite was 5.0 g, and the reaction liquid was 1.0 L. At these conditions, the yield of the product was calculated by the following eqn (2).

$$\text{Yield} = C \div (4\ \text{g/1 L}) \times 100\% \quad (1)$$

$$\text{Yield} = C \div (5\ \text{g/1 L}) \times 100\% \quad (2)$$

C – concentration of graphene dispersion ($g\ L^{-1}$).

3. Results and discussion

3.1 Graphite exfoliation in various electrolyte systems

To compare the effects of different electrolyte systems on the exfoliation of graphite to produce graphene, experiments with sodium chloride, sodium hydroxide, PVP, SDBS and DTAB as electrolytes were carried out. The experiments were performed at an electrolyte concentration of 5.0%, air flow of 1.0 L h^{-1}, applied current strength of 10 mA, graphite dosage of 4.0 g and reaction time of 3 h.

The XRD results are shown in Fig. 2. Fig. 12 shows that there are two characteristic peaks in the XRD pattern of the graphene product (around $2\theta = 27°$ and $2\theta = 54°$), indicating that the product has carbon-based material composition and internal carbon atoms or a molecular structure.[32,33,44,45] This indicated that the five electrolytes have an effect on exfoliation while forming graphene by our method. Visibly, the positions of the characteristic XRD peaks for the products obtained from

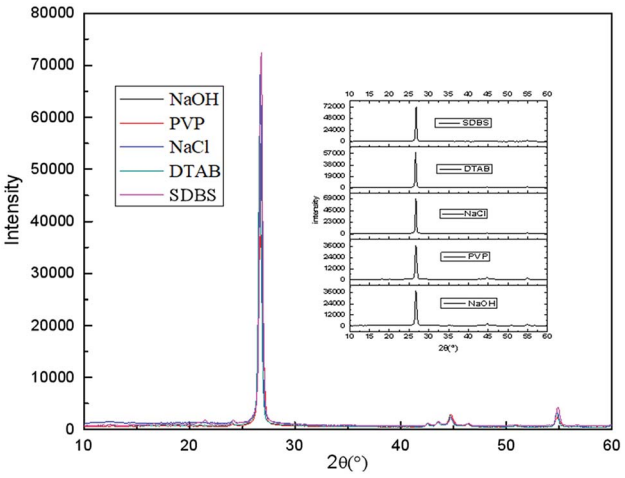

Fig. 2 XRD patterns of the products obtained from different electrolytes.

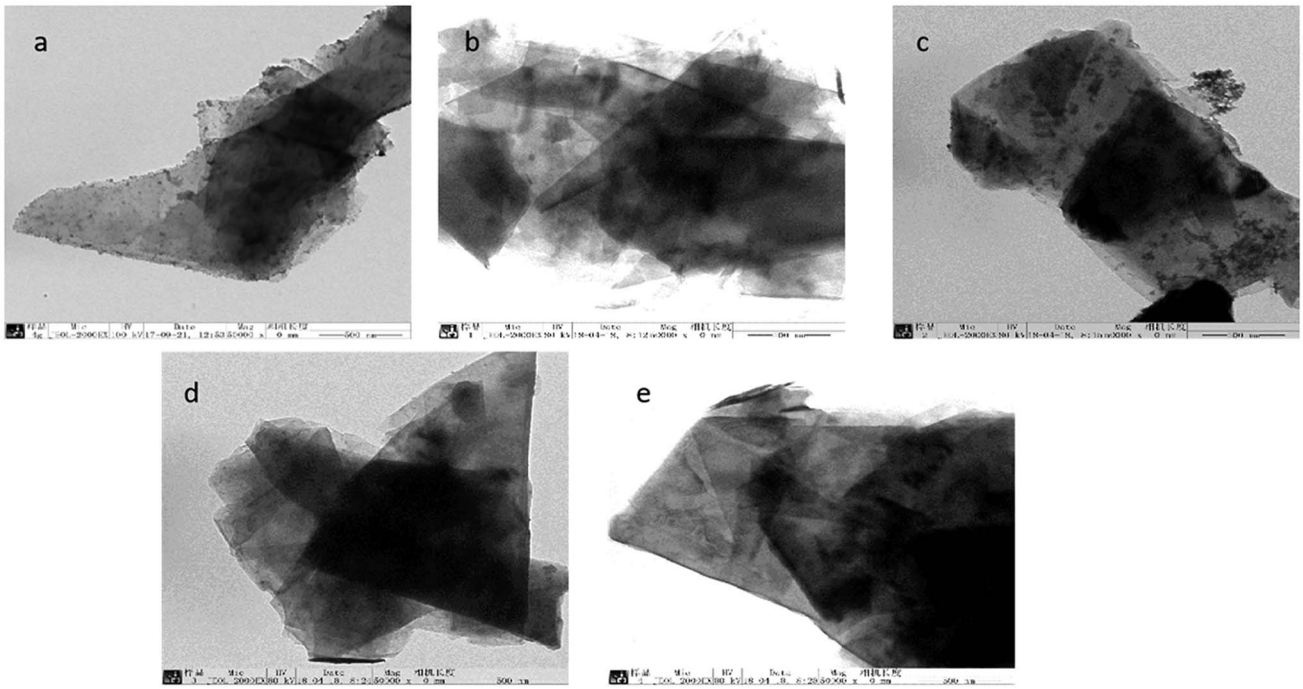

Fig. 3 TEM images of the samples produced with (a) sodium chloride; (b) sodium hydroxide; (c) PVP; (d) SDBS and (e) DTAB as the electrolytes.

different electrolytes did not shift, illustrating that the electrolytes did not change the internal structure of the product. The TEM images in Fig. 3 display that the samples obtained using different electrolytes possess the characteristic features of a thin-layer graphene sheet, which indicates that graphite is successfully exfoliated into a uniform thin layer of graphene. Fig. 4 and 5 show the FT-IR and Raman diagrams, respectively. The key absorption peaks of graphene were observed. The strength of the absorption peaks of graphene products in sodium hydroxide and PVP electrolyte systems were significantly weaker than those observed for the other 3 electrolyte systems. This result was obtained due to the following reasons: the addition of sodium hydroxide can increase the oxygen precipitation side effect in the anode[46,47] to hinder the generation of hydroxyl radicals; also, PVP is poorly hydrophilic, which is not conducive to the uniform dispersion of graphite in the system. Meanwhile, the absorption peaks of the products with DTAB as the electrolyte were weaker than those with sodium chloride and SDBS. Although the three electrolytes were strongly hydrophilic, the solubilities at 20 °C were 13 g L^{-1}, 362 g L^{-1} and 100 g L^{-1}, respectively. As DTAB is relatively less hydrophilic, it was not favorable for the formation of hydroxyl radicals. The absorption peak strength of the product with SDBS as the electrolyte was stronger than that in the sodium chloride system. On one hand, this was because SDBS is an anionic surfactant with good electrical conductivity, which is favorable

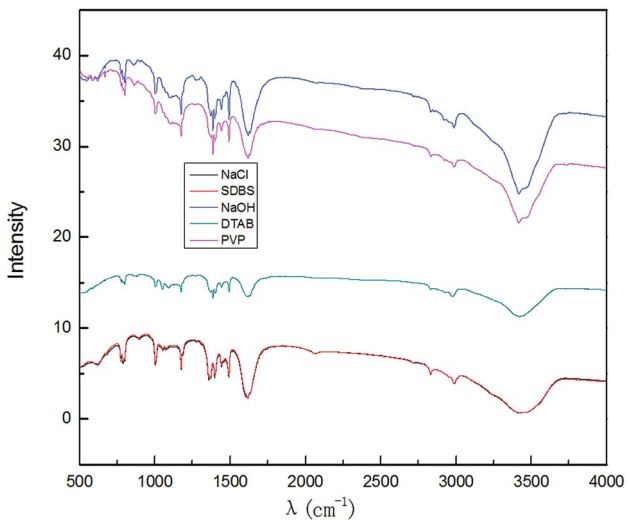

Fig. 4 FT-IR patterns of the products obtained from different electrolytes.

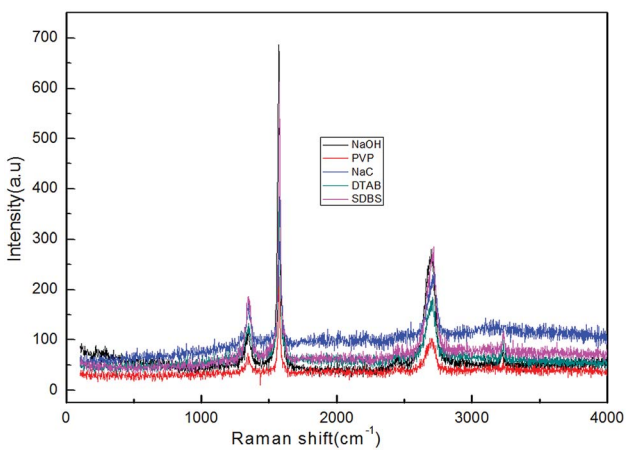

Fig. 5 Raman spectra of the products obtained from different electrolytes.

for the formation of hydroxyl radicals and it can avoid the corrosive effect of the salt electrolyte. On the other hand, SDBS is strongly hydrophilic, which enables even dispersion of graphite in the system. Therefore, these two effects facilitated the exfoliation of graphite to form good-quality graphene. Meanwhile, the anions generated during the ionization in water ensured the charge balance in the solution. In summary, SDBS is the best electrolyte for our method. We further studied the effects of process parameters on exfoliation in the SDBS electrolyte system.

3.2 Optimization of process parameters

3.2.1 Effect of exfoliation time. The conditions to study the effects of exfoliation times on the exfoliation process were set as follows: the concentration of the SDBS solution was 5.0% (w/v), the air flow was 1.0 L h^{-1}, the applied current strength was 10 mA, the dosage of graphite powder was 3.0 g and the exfoliation times ranged between 1 h and 15 h. The FT-IR result is shown in Fig. 6. It can be seen that the main absorption peaks of the samples obtained by different exfoliation times were at 1045 cm^{-1}, 1264 cm^{-1}, 1512 cm^{-1}, 1620 cm^{-1} and 3400 cm^{-1}. The characteristic peaks at 1264 cm^{-1} and 1512 cm^{-1} were assigned to the C–O–C vibration absorption peak[48,49] and the stretching of the C–O bond.[50,51] The peak at 1045 cm^{-1} was caused by the C–OH vibration.[52] Moreover, the transmittance peak appearing at the wave number of 1620 cm^{-1} corresponded to the sp^2 structure of the graphite crystal C=C stretching vibration peak.[53] The broad and strong absorption peak in the fingerprint regions around 3000–3700 cm^{-1} could be attributed to hydroxyl stretching vibration.[48,51] These results further indicated that the preparation method introduced hydroxyl radicals into graphene without changing the carbon-based structure. Fig. 6 shows that when the time was extended, the intensity of the characteristic peak of graphene first increased and then decreased and reached the maximum at 3 h. This is due to the synergistic effect of electrical exfoliation and oxidation of hydroxyl radicals. At the beginning, more hydroxyl radicals were produced with the increase in time, enhancing the synergistic effect. However, when the time was prolonged, graphene restacking was more pronounced. This resulted in decrease in the intensity of the characteristic peaks. Therefore, the appropriate reaction time was 3 h, and the subsequent experiments were carried out for 3 h.

3.2.2 Effect of SDBS solution concentration. The effect of the electrolyte concentration on the preparation of graphene was studied at its concentration from 1.0% (w/v) to 10.0% (w/v); the air flow rate was 1.0 L h^{-1}, the applied current strength was 10 mA, and the dosage of the graphite powder was 3.0 g. The results are shown in Fig. 7.

It can be easily seen from Fig. 7 that the intensity of the graphene characteristic peak increased as the electrolyte concentration was increased; it reached the maximum at 10.0% (w/v) and then decreased. This phenomenon can be attributed to the increase in the conductivity of the solution when a higher concentration of electrolyte is used. Good electrical conductivity leads to good ·OH formation and a better synergistic effect with electrical exfoliation. Furthermore, the solubility of SDBS at 20 °C was 100 g L^{-1}, and the conductivity did not continue to increase when the solution was saturated at a higher electrolyte concentration; this indicated that the generation of hydroxyl radicals did not increase, and excess undissolved SDBS was not conducive to the dispersion of graphite in the system, due to which the intensity of the characteristic peak of graphene decreased. Therefore, when the electrolyte concentration was less than 10.0% (w/v), the increase in the conductivity was dominant; when the concentration exceeded 10.0% (w/v), the reduction in hydroxyl radicals contributed more and was predominant. The selection of optimal electrolyte concentration for the generation of hydroxyl radicals in different electrolyte systems by different production methods is also reported in literatures.[54–57] Therefore, it is reasonable to expect that an optimal concentration of the electrolyte may exist. Meanwhile, SDBS is a clean anionic surfactant; it has almost no corrosion for the electrodes at higher concentrations. As can be inferred from the results, 10.0% (w/v) electrolyte concentration was found to be suitable for the investigation.

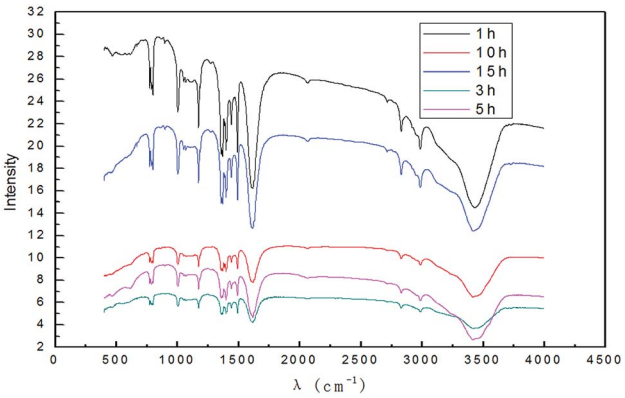

Fig. 6 FT-IR patterns of the products obtained with different reaction times.

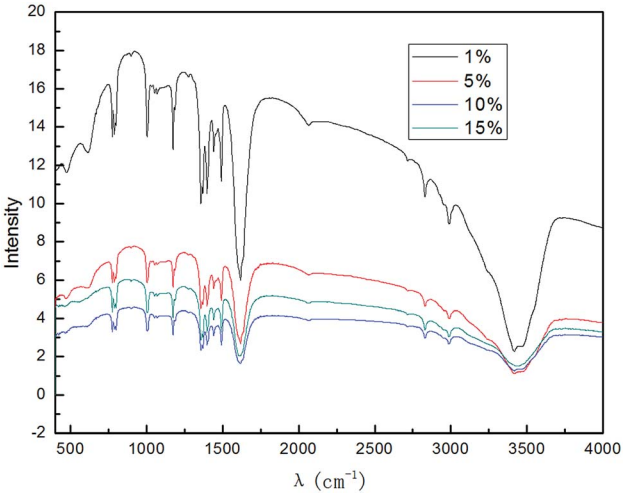

Fig. 7 FT-IR patterns of the products obtained with various electrolyte concentrations.

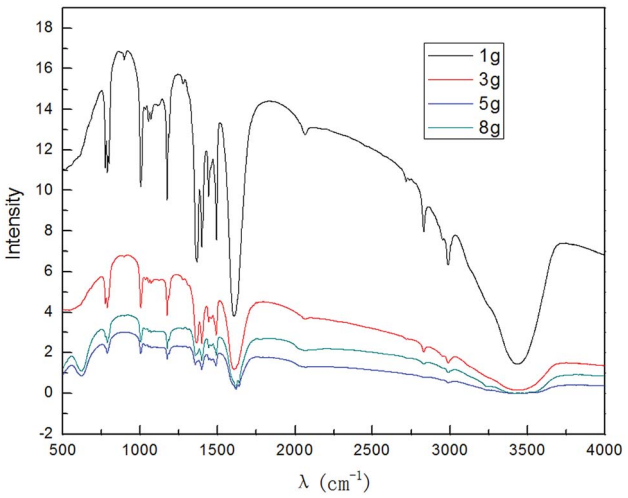

Fig. 8 FT-IR patterns of the products obtained with different graphite dosages.

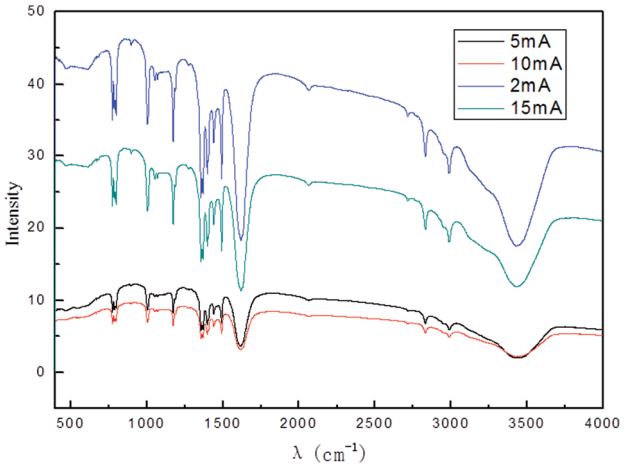

Fig. 9 FT-IR patterns of the products obtained with different direct current strengths.

3.2.3 Effect of graphite dosage. The dosage of graphite is a key parameter because graphite is not only the raw material for the reaction, but also acts as a catalyst for the process. Fig. 8 shows the effect of the graphite dosage on the exfoliation of graphene at an air flow of 1.0 L h^{-1} and applied current strength of 10 mA; the dosage of the graphite powder was changed from 1.0 g to 8.0 g.

As can be seen from Fig. 8, as the amount of graphite was increased, the peak intensity of graphene increased first and reached the maximum at 5.0 g; then, it decreased. This is because higher dosage of graphite resulted in better catalytic activity, which led to an increase in the intensity of the characteristic peaks of graphene. At the same time, the higher the dosage of graphite, the higher the restacking of graphene and its uneven dispersion, which resulted in decrease in the characteristic peak intensity of graphene. From the results, the suitable dosage of graphite was found to be 5.0 g.

3.2.4 Effect of applied current strength. Fig. 9 shows the effects of the applied current strength on the exfoliation process. The applied current strength was adjusted from 2 mA to 15 mA.

The result in Fig. 9 shows that when the applied current intensity was increased, the intensity of graphene characteristic peak first increased, achieved a maximum at 10 mA and then decreased. This may be due to the combination of hydroxyl radical exfoliation and electrical exfoliation. Within a certain range, a relatively higher applied current intensity, indicating a higher power input, can result in higher hydroxyl radical generation and better electrical exfoliation effects. However, when the current is very high, the cathode and the anode will have hydrogen and oxygen precipitation side reactions.[58,59] The reactions are given as (3) and (4). Bipolar side effects can lead to decrease in hydroxyl radical production, current efficiency and the effect of electrical exfoliation.

$$2H_2O - 4e \rightarrow O_2\uparrow + 4H^+ \quad (3)$$

$$2H^+ + 2e \rightarrow H_2\uparrow \quad (4)$$

To ensure better exfoliation, 10 mA was applied as the suitable applied current strength.

3.2.5 Effect of the air flow. Generally, a higher air flow allows the graphite to be more uniformly dispersed in the solution and facilitates better contact of graphite with the produced ·OH, thereby improving the preparation. From an economical point of view, the use of high air flow is not considered as cost effective due to high operating costs and energy consumption. The effect of the air flow rate on graphene exfoliation is shown in Fig. 10. The experiments were carried out under the above-mentioned optimum conditions. From Fig. 10, it can be seen that the intensity of the characteristic peak of graphene first increased with increasing air flow up to the maximum at 1.0 L h^{-1} and then decreased. This was because a higher air flow could initially accelerate the mass transfer rate and the ·OH formation; however, when the air flow was very high, the mass transfer interfacial area decreased at

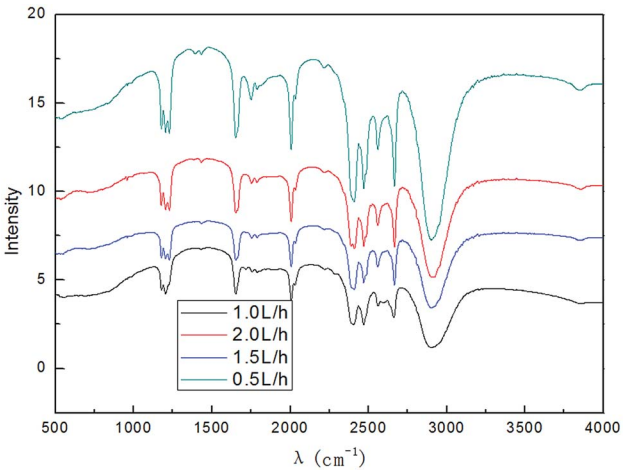

Fig. 10 FT-IR patterns of the products obtained with various air flows.

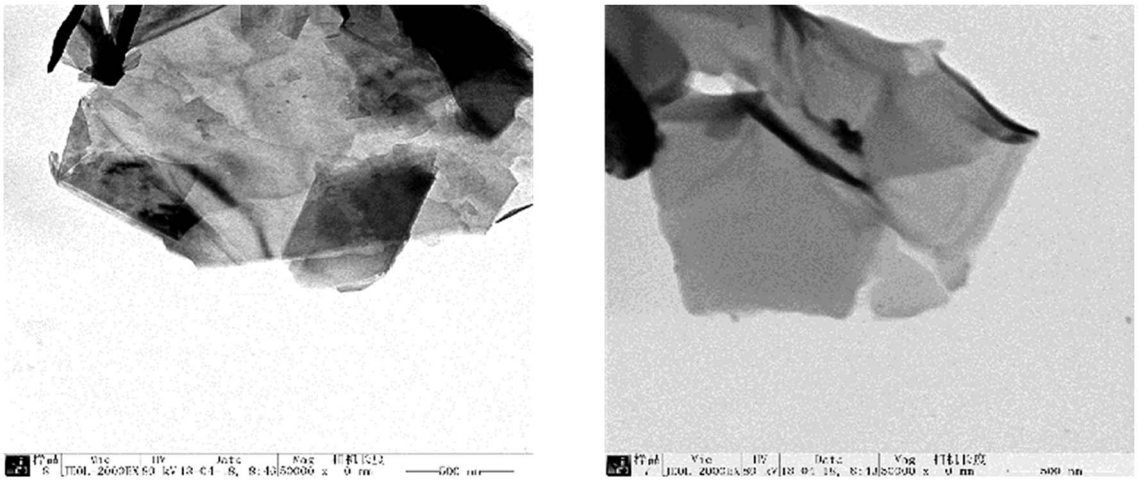

Fig. 11 TEM images of the samples produced at optimum conditions.

unit time. This was not favorable for ·OH formation and mass transfer rate, leading to decrease in the strength of the characteristic peak of graphene. Hence, the air flow of 1.0 L h^{-1} was selected.

In summary, the optimal exfoliation conditions of graphene were as follows: SDBS electrolyte concentration, 10.0% (w/v); graphite dosage, 5.0 g; exfoliation time, 3 h; applied current strength, 10 mA; air flow, 1.0 L h^{-1}.

3.3 Mechanism discussion

3.3.1 Transmission electron microscopy (TEM) analysis. To investigate the mechanism of the method, the structural change in the graphene product obtained under optimum exfoliation conditions was observed using a transmission electron microscope.

The results are shown in Fig. 11. As can be seen from Fig. 11, the presence of wrinkles and folds on the sheet is the characteristic feature of thin-layer graphene sheets,[60] which indicates that graphite was successfully exfoliated into a uniform thin layer of graphene.

3.3.2 X-ray diffraction (XRD) analysis. The exfoliation degree of the graphene product obtained by the method was studied by X-ray diffraction (Fig. 12); the XRD pattern of graphite is also presented in this figure. Fig. 12 shows that there are two characteristic peaks in the XRD pattern of the graphene product (around $2\theta = 27°$ and $2\theta = 54°$), which were assigned to the (002) plane.[60–63] The graphene product exhibited almost the same diffraction peak as graphite, which indicated that graphene still retained the structure of carbon atoms or molecules; however, the diffraction peak broadened and the intensity weakened. This is because the size of the layer became smaller when graphite was transformed to graphene.[48] The result of the XRD analysis was in good agreement with that of TEM analysis.

3.3.3 Raman spectroscopy (Raman) analysis. Structural changes during the oxidation and exfoliation process can be observed by Raman spectroscopy. Fig. 13 shows the Raman spectra of the graphene product. As can be seen, Raman peaks at 1351 cm^{-1}, 1582 cm^{-1}, 2720 cm^{-1} and 3250 cm^{-1} are graphene's characteristic peaks, which can be attributed to the D, G, D′(2D) and G′ modes, respectively. The G and D peaks were

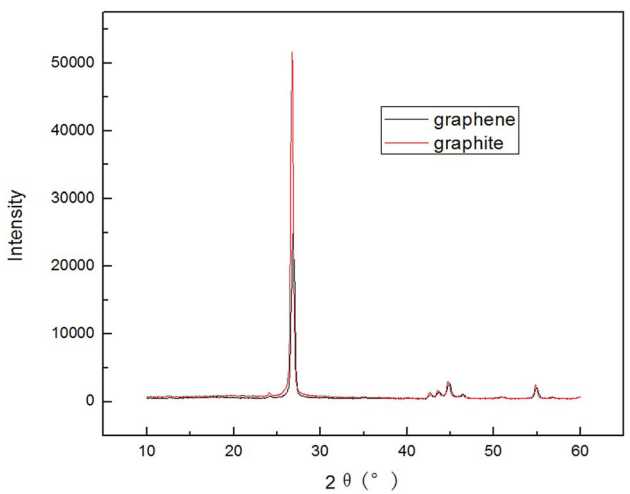

Fig. 12 XRD patterns of raw materials and the graphene product.

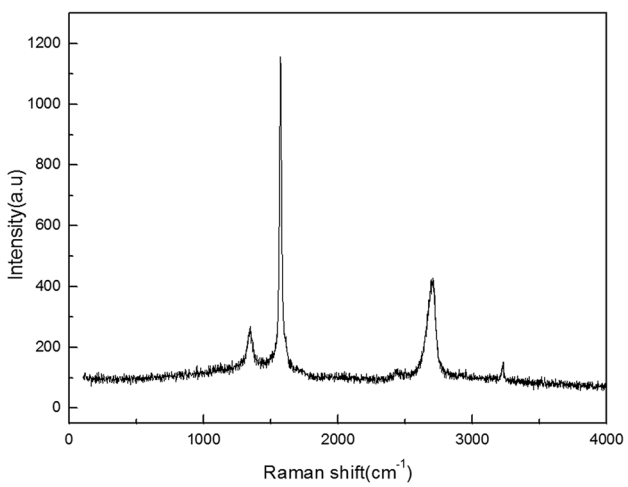

Fig. 13 Raman pattern of the graphene product.

due to the sp^2 structure. The G peak was due to the stretching motion of all sp^2 atom pairs in the carbon ring or long chain.[60,63] The D peak was produced by the sp^2 atom's respiratory vibration mode in the carbon ring, which indicated that some sp^2 hybridized carbon atoms in the structure were converted to sp^3 hybrid structures. This transformation may destroy the C=C double bond in the graphite layer. In addition, the intensity ratio of the G band to the D band also represents the sp^2/sp^3 carbon atom ratio.[64,65] As can be seen from Fig. 13, the intensity of the G band is much stronger than that of the D band, indicating that the carbon skeleton structure has not changed. This is very consistent with the FT-IR analysis. D′(2 D) and G modes belong to the sum and the frequency of the unordered Raman mode, and Raman allows the presence of intact graphite crystals and defects. Graphene has a low degree of graphitization. Therefore, D′ (2D) and G′ modes are usually very weak and wide. The second-order Raman peak was not considered here.[51] The graphene absorption peak at 2720 cm^{-1} shifted slightly at different layers. Femri *et al.*[66] studied the change in the 2D peak position with the number of layers of graphene and used the double resonance model to explain this phenomenon. To further investigate the number of layers of graphene products, AFM analysis was used.

3.3.4 Atomic force microscopy (AFM). Atomic force microscopy is the most direct and effective method to characterize graphene materials. The use of AFM makes it possible to observe single-layer graphene. The thickness of graphene is only 0.335 nm; thus, it is difficult to observe it by SEM, but it can be clearly observed by AFM. Geim *et al.*[6] found that a single graphene attached to the surface of a Si wafer and a certain thickness (300 m) of SiO_2 layer can be clearly observed under an atomic force microscope. To further identify the number of layers of the graphene products by different electrolyte systems, AFM analysis was used; the results are shown in Fig. 14. From Fig. 14(a)–(d), it can be seen that the thicknesses of the graphene products obtained using sodium hydroxide, PVP, DTAB and sodium chloride as electrolytes are 9 nm, 7 nm, 1.6 nm and 1.1 nm, respectively, which indicate that the layer numbers of the graphene products are 30, 20, 4 and 3. From Fig. 14(e), it can be seen that the thickness of the graphene product obtained using SDBS electrolyte is 0.6 nm, which shows that the layer number of the graphene product is about 2. The AFM result showed that the quality of graphene is good, which can be attributed to the synergistic effect between the strong oxidation of hydroxyl radicals and electrical exfoliation. The schematic representation of the exfoliation mechanism can be seen in Fig. 15. The method has the advantages of simplicity, mild preparation conditions, no use of aggressive reagents, recycling of the reaction medium, *etc.* Thus, it can be an alternative green and efficient method for the production of graphene and graphene derivatives in industry.

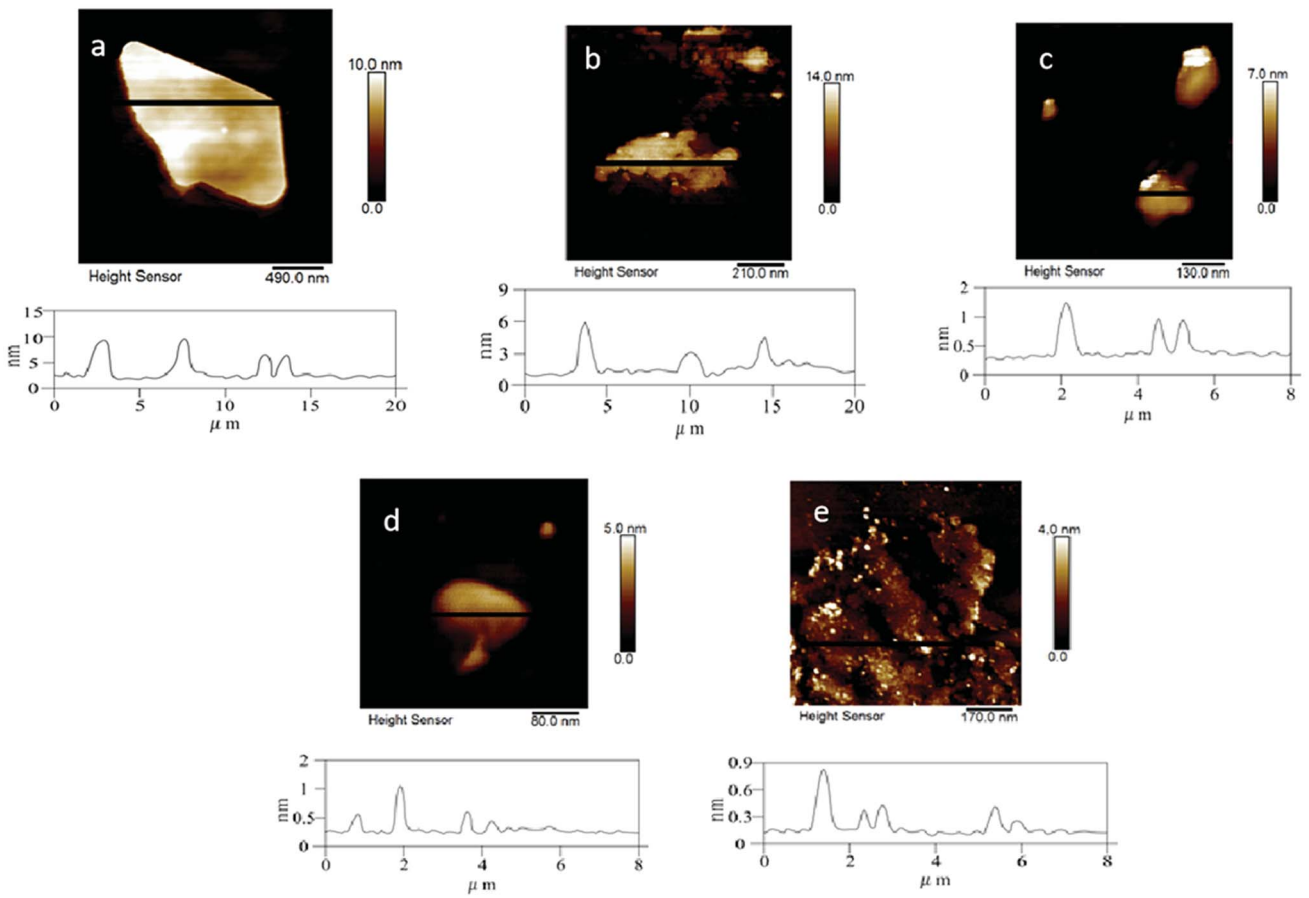

Fig. 14 AFM images of the samples obtained with (a) sodium hydroxide; (b) PVP; (c) DTAB; (d) sodium chloride and (e) SDBS as the electrolytes.

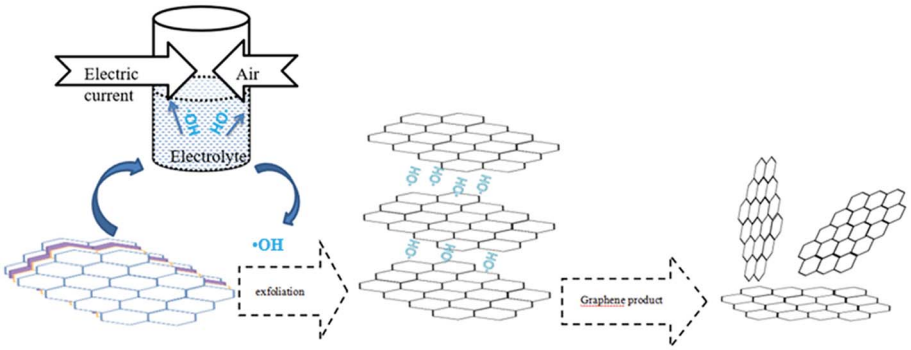

Fig. 15 Schematic representation of the exfoliation mechanism.

3.4 Yield of the production

The experiments with sodium hydroxide, PVP, DTAB, sodium chloride and SDBS as the electrolytes were carried out under the conditions mentioned in Section 3.1. The experiment with SDBS as the electrolyte under optimal conditions was also carried out. The concentrations of the graphene dispersions obtained from sodium hydroxide, PVP, DTAB sodium chloride and SDBS electrolytes were measured to be 1.313 g L^{-1}, 1.360 g L^{-1}, 1.811 g L^{-1}, 3.102g L^{-1} and 3.341 g L^{-1}, respectively. The concentration of the graphene dispersion obtained by the SDBS system under optimal conditions was 4.485 g L^{-1}. The yields of the graphene products in sodium hydroxide, PVP, DTAB, sodium chloride and SDBS electrolyte systems were 32.9%, 34.0%, 45.2%, 77.5% and 83.5%, respectively. The yield of the graphene product in the SDBS system under optimal conditions was 89.7%.

3.5 Recycling of the electrolyte

To study the effect of the reuse of electrolyte, we collected and recycled the electrolyte after the experiment. All the experiments were performed at optimal exfoliation conditions: SDBS electrolyte concentration, 10.0% (w/v); graphite dosage, 5.0 g; exfoliation time, 3 h; the applied current strength, 10 mA; air flow, 1.0 L h^{-1}. The results of the electrolyte recycling for 3 times are shown in Fig. 16.

It can be seen from Fig. 16 that the main absorption peaks are the same, which indicates that the electrolyte can be recycled and used. However, the absorption peaks of the products after recycling 2 times and 3 times were slightly weakened because of the loss of electrolyte during recycling. The recyclability of the electrolyte further proves that our production method can be a green and potential method for graphene production in industry.

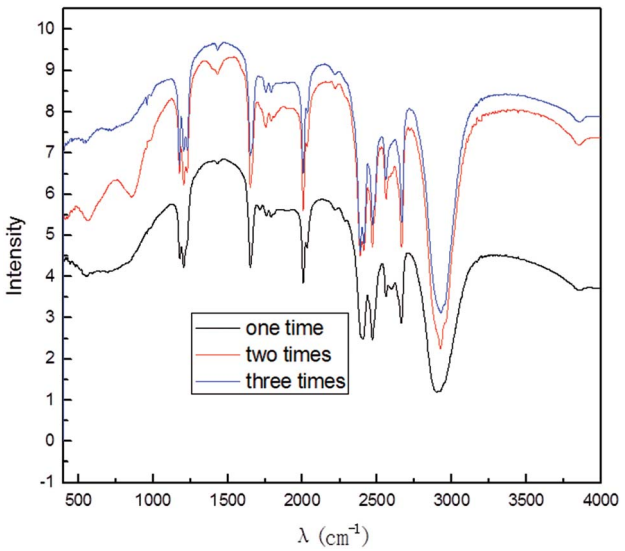

Fig. 16 FT-IR patterns of the graphene product obtained with different electrolyte recycling times.

4. Conclusion

In this work, we investigated a new method by the combination of hydroxyl radicals and electrical exfoliation to produce graphene from graphite. The roles of various electrolyte systems (sodium hydroxide, PVP, DTAB, sodium chloride and SDBS) for the exfoliation of graphite were investigated. The yields of the graphene products in sodium hydroxide, PVP, DTAB, sodium chloride and SDBS electrolyte systems were 32.9%, 34.0%, 45.2%, 77.5% and 83.5%, respectively, with SDBS showing the best exfoliation effect. The obtained optimal process parameters were as follows: graphite dosage, 5.0 g; SDBS solution concentration, 10.0% (w/v); applied current strength, 10 mA; air flow, 1.0 L h^{-1}; and exfoliation time, 3 h. Under optimal conditions, the yield of the graphene product was 89.7%. Under optimal conditions, the layer number of the graphene product was about 2, while those of the products of sodium hydroxide, PVP, DTAB and sodium chloride systems were 30, 20, 4 and 3, respectively, at the same experimental conditions. The good quality of graphene could be attributed to good electrical conductivity and excellent hydrophilic properties of SDBS, which were favorable for the formation of hydroxyl radicals and enabled even dispersion of graphite. These two effects facilitated the exfoliation of graphite to form good-quality graphene. SDBS as the electrolyte did not corrode the electrode, and it could be recycled; also, it does not pollute the environment and reduces the production cost, which is favorable for mass production.

Conflicts of interest

There are no conflicts to declare.

Acknowledgements

We are grateful to the Materials Advanced Research Institute for their test supports in the process of characterization.

References

1 X. Li, W. F. Zhao, *et al.*, Preparation and Characterization of Graphene, *Mater. Lett.*, 2008, **22**(8), 48.
2 F. Liu and P. B. Ming, Ambition calculation of ideal strength and phonon instability of graphene in tension, *Phys. Rev. B: Condens. Matter Mater. Phys.*, 2007, **76**(6), 064120.
3 R. R. Nair, P. Blake, *et al.*, Fine structure constant defines visual transparency of grapheme, *Science*, 2008, **320**, 1308.
4 S. Sindhu, K. Shishir, *et al.*, Million-fold decrease in polymer moisture permeability by a graphene monolayer, *ACS Nano*, 2016, 1–26.
5 B. Seger and P. V. Kamat, Electro catalytically active graphene-platinum nanocomposites role of 2-D carbon support in pem fuel cells, *J. Phys. Chem.*, 2009, **113**(19), 7990.
6 K. S. Novoselov and A. K. Geim, *et a1.*, Electric field effect in atomically thin carbon films, *Science*, 2004, **306**, 666–669.
7 M. D. Stoller and S. J. Park, *et a1.*, Graphene-based ultra capacitors, *Nano Lett.*, 2008, **8**, 3498–3502.
8 J. C. Meyer, A. K. Geim, *et al.*, The structure of suspended graphene sheets, *Nature*, 2007, **446**(7131), 60–63.
9 J. C. Meyer, A. K. Geim, *et al.*, On the roughness of single-and bi-layer graphene membranes, *Solid State Commun.*, 2007, **143**(1–2), 101–109.
10 A. Fasolino, J. H. Los, *et al.*, Intrinsic ripples in grapheme, *Nat. Mater.*, 2007, **6**(11), 858–861.
11 C. Knieke and K. Berger, *et a1.*, Scalable production of graphene sheets by mechanical delimitation, *Carbon*, 2010, **48**(11), 3196–3204.
12 D. Sha, X. D. Qi, *et al.*, A facile way to large-scale production of few-layered graphene *via* planetary ball mill, *Chin. J. Polym. Sci.*, 2016, **34**(10), 1270–1280.
13 G. R. Kumar, K. Jayasankar, *et al.*, Shear-force-dominated dual-drive planetary ball milling for scalable production of graphene and its electro catalytic application with Pd nanostructures, *RSC Adv.*, 2016, **6**(24), 20067–20073.
14 H. H. Zhu, Y. L. Cao, *et al.*, One-step preparation of graphene nanosheets *via* ball milling of graphite and the application in lithium-ion batteries, *J. Mater. Sci.*, 2016, **51**(8), 3675–3683.
15 K. S. Kim, Y. Zhao, *et al.*, Large-scale pattern growth of graphene films for stretchable transparent electrodes, *Nature*, 2009, **457**(7230), 706–710.
16 A. Reina, X. T. Jia, *et al.*, Large area, few-layer graphene films on arbitrary substrates by chemical vapor deposition, *Nano Lett.*, 2009, **9**(1), 30–35.
17 X. S. Li, W. W. Cai, *et al.*, Large-area synthesis of high-quality and uniform graphene films on copper foils, *Science*, 2009, **324**(5932), 1312–1314.
18 X. S. Li, W. W. Cai, *et al.*, Evolution of graphene growth on Ni and Cu by carbon isotope labeling, *Nano Lett.*, 2009, **9**(12), 4268–4272.
19 J. Zheng, C. A. Di, *et al.*, High quality graphene with large flakes exfoliated by oley amine, *Chem. Commun.*, 2010, **46**(31), 5728–5730.
20 T. V. Khaia, D. S. Kwaka, *et al.*, Direct production of highly conductive graphene with low oxygen content by a microwave-assisted solvothermal method, *Chem. Eng. J.*, 2013, **232**(9), 346–355.
21 F. S. Al-Hazmi, G. H. Al-Harbi, *et al.*, One pot synthesis of graphene based on microwave assisted solvothermal technique, *Synth. Met.*, 2015, **200**, 54–57.
22 Y. Hemandez, V. Nicolosi, *et al.*, High-yield production of graphene by liquid-phase exfoliation of graphite, *Nat. Nanotechnol.*, 2008, **3**(9), 563–568.
23 X. L. Li, G. Y. Zhang, *et al.*, Highly conducting graphene sheets and langmuir-blodgett films, *Nat. Nanotechnol.*, 2008, **3**(9), 538–542.
24 C. A. Amarnath and C. E. Hong, *et a1.*, Efficient synthesis of graphene sheets using pyrrole as a reducing agent, *Carbon*, 2011, **49**(11), 3497–3502.
25 Y. Y. Shao and J. Wang, *et a1.*, Facile and controllable electrochemical reduction of graphene oxide and its applications, *J. Mater. Chem.*, 2010, **20**(4), 743–748.
26 H. L. Guo and X. F. Wang, *et a1.*, A Green Approach to the Synthesis of Graphene Nanosheets, *ACS Nano*, 2009, **3**(9), 2653–2659.
27 W. C. Soon, W. L. Chin, *et al.*, Green preparation of reduced graphene oxide using a natural reducing agent, *Ceram. Int.*, 2015, **41**, 9505–9513.
28 G. A. Tai, T. Zeng, *et al.*, Temperature and pH effect on reduction of graphene oxides in aqueous solution, *Mater. Res. Express*, 2014, **1**(3), 37–40.
29 O. Mondal, S. Mitra, *et al.*, Reduced graphene oxide synthesis by high energy ball milling, *Mater. Chem. Phys.*, 2015, **161**, 123–129.
30 S. K. Sahoo and A. Mallik, Simple, fast and cost-effective electrochemical synthesis of few layer graphene nanosheets, *Nano*, 2015, **10**(2), 3807–3809.
31 M. Min, M. M. Wang, *et al.*, Simultaneous electrochemical synthesis of few-layer graphene flaks on both electrodes in portico ionic liquids, *Chem. Commun.*, 2013, **49**(46), 5301–5303.
32 M. H. Chakrabarti, N. S. A. Manan, *et al.*, One-pot electrochemical gram-scale synthesis of graphene using deep eutectic solvents and acetonitrile, *Chem. Eng. J.*, 2015, **274**, 213–223.
33 N. Azbar, T. Yonar, *et al.*, Comparison of various advanced Oxidation processes and chemist treatment methods for COD and color removal from a polyester and acetate fiber dyeing effluent, *Chemosphere*, 2004, **55**(1), 35–43.

34 X. J. Ma, Y. Q. Cong, *et al.*, Electrochemical induced hydroxyl radical degradation of phenolic pollutants in water, *J. Chem. Ind.*, 2008, **59**(1), 60–63.
35 H. F. Sun and J. Q. Du, Application of Hydroxyl Radical Active Oxygen in High Concentration Organic Wastewater Treatment, *Mod. Chem. Ind.*, 2010, **30**(1), 102–105.
36 W. Li, Chemical Modification of Carbon Nanotubes with Hydroxyl Radical, MPhil thesis, East China Normal University, ShangHai, 2005.
37 G. Feng, P. Cheng, *et al.*, Accelerated crystallization of zeolites *via* hydroxyl free radicals, *Science*, 2016, **351**(6278), 1188–1191.
38 L. Zhang and X. Wang, *The method and apparatus for the preparation of graphene from graphite*, CN201811179420.5, 2018.10.10.
39 E. C. Ou, Preparation of graphene dispersion and its free organization, MPhil thesis, Hunan University, Hunan, 2012.
40 M. Lotya, P. J. King, *et al.*, High-Concentration, Surfactant-Stabilized Graphene Dispersions, *ACS Nano*, 2010, **4**(6), 3155–3162.
41 Y. N. Cai, C. Yu, *et al.*, Study on Dispensability of Graphene Aqueous Solution, *J. Mater. Sci.*, 2014, 11.
42 Z. F. Ma, Z. D. Yang, *et al.*, Research progress of graphene-based super capacitors, *Science and Energy Storage Technology*, 2014, **1**(3), 49–51.
43 W. S. Yang, L. Zhang, *et al.*, Progress in research on preparation and application of graphene composites, *J. Mater. Eng.*, 2015, **43**(3), 91–97.
44 U. Khan, A. O'Neil, *et al.*, High-Concentration Solvent Exfoliation of Graphene, *Small*, 2010, **6**(7), 864–871.
45 M. Min, M. M. Wang, *et al.*, Simultaneous electrochemical synthesis of few-layer graphene flaks on both electrodes in protic ionic liquids, *Chem. Commun.*, 2013, **49**(46), 5301–5303.
46 M. N. Schuchmann and C. V. Sonntag, Hydroxyl Radical-Induced Oxidation of 2-Methyl-2-propanol In Oxygenated Aqueous Solution. A Product and Pulse Radiolysis Study, *J. Phys. Chem.*, 1979, **83**(7), 780–784.
47 J. M. Chen, W. W. Pan, *et al.*, Research Progress on the Mechanism and Detection of Hydroxyl Radicals in Electrochemical System, *J. Zhejiang Univ. Technol.*, 2008, **36**(4), 416–422.
48 W. S. Ma, *et al.*, Preparation and Characterization of Graphene, *J. Chem. Eng. Chin. Univ.*, 2010, **24**(4), 719–722.
49 H. He, J. Klinowski and A. Lcrf, *et a1.*, A new structural model for graphite oxide, *Chem. Phys. Lett.*, 1998, **2870**(2), 53–56.
50 X. X. Ma, Enzymatic Hydrolysis of Natural Cellulose, MPhil thesis, Beijing Chemical University, Beijing, 2010.
51 L. L. Wang, G. T. Han, *et al.*, Comparative study of composition, structure and properties of *Apocynum venetum* fibers under different pretreatments carbohyder, *Polymer*, 2007, **69**, 391–397.
52 Y. H. Yang, H. J. Sun, *et al.*, Preparation and Characterization of Graphene by Redox, *Chin. J. Inorg. Chem.*, 2010, **26**(11), 2083–2090.
53 K. Bissessur and S. F. Scully, Intercalation of solid polymer electrolytes into graphite oxide, *Solid State Ionics*, 2007, **178**(11–12), 877–882.
54 J. Lee, N. Koo, *et al.*, Reactive oxygen species, aging, and ant oxidative nutraceuticals, *Compr. Rev. Food Sci. Food Saf.*, 2004, **3**, 21–33.
55 C. Li, *et al.*, *Hydroxyl radical generating device and its using method*, China, CN 104496003 A, 2015.
56 M. Zhang, Hydroxyl radicals react with inorganic ox acids, MPhil thesis, Dalian Maritime University, Dalian, 2015.
57 M. Jiang, Study on the Influence of Electrochemical Detection of Hydroxyl Free Radicals and Generations, PhD thesis, Xi'an University of Architecture and Technology, Xi'an, 2015.
58 K. Bissessur and S. F. Scully, Intercalation of solid polymer electrolytes into graphite oxide, *Solid State Ionics*, 2007, **178**(11–12), 877–882.
59 S. Hummers and R. Offeman, Preparation of graphitic oxide, *J. Am. Chem. Soc.*, 1958, **80**(6), 1339.
60 J. Wang and Z. D. Han, The combustion behavior of polyacrylate ester graphite oxide composites, *Polym. Adv. Technol.*, 2006, **17**(4), 335–340.
61 P. J. Yen, C. C. Ting, *et al.*, Facile production of graphene nanosheets comprising nitrogen-doping through *in situ* cathodic plasma formation during electrochemical exfoliation, *J. Mater. Chem. C*, 2017, **5**, 2597–2602.
62 C. C. Yang, M. H. Tsai, *et al.*, Carbon nanotube/nitrogen-doped reduced Graphene oxide nanocomposites and their application in supercapacitors, *J. Nanosci. Nanotechnol.*, 2017, **17**, 5366–5373.
63 L. J. Li, C. W. Chu, *et al.*, Plasma-assisted electrochemical exfoliation of graphite for rapid production of graphene sheets, *RSC Adv.*, 2014, **4**, 6946–6949.
64 C. A. Ferrari and J. Robertson, *Phys. Rev. B: Condens. Matter Mater. Phys.*, 2000, **61**(20), 14095–14107.
65 C. Gomez-Navarro, R. T. Weitz, *et al.*, Electronic transport properties of individual chemically reduced graphene oxide sheets, *Nano Lett.*, 2007, **7**(11), 3499–3503.
66 A. C. Femri, J. C. Meyer, *et al.*, A Study on Graphene-Metal Contact, *Phys. Rev. Lett.*, 2006, **97**(18), 7401.